THE JOURNAL OF BIOLOGICAL CHEMISTRY VOL. 283, NO. 25, pp. 16985–16992, June 20, 2008

The M1P1 Loop of TASK3 K2P Channels Apposes the Selectivity Filter and Influences Channel Function*

Received for publication, February 20, 2008, and in revised form, April 15, 2008 Published, JBC Papers in Press, April 16, 2008, DOI 10.1074/jbc.M801368200

Catherine E. Clarke[‡1,2], **Emma L. Veale**[§¶1], **Ken Wyse**[‡], **Jamie I. Vandenberg**[‡], **and Alistair Mathie**[§¶3]

From the [§]*Medway School of Pharmacy, Universities of Kent and Greenwich at Medway, Central Avenue, Chatham Maritime, Kent ME4 4TB, United Kingdom,* [¶]*Biophysics Section, Blackett Laboratory, Division of Cell and Molecular Biology, Imperial College London, Exhibition Road, London SW7 2AZ, United Kingdom, and* [‡]*Victor Chang Research Institute, University of New South Wales, Sydney, New South Wales 2010, Australia*

Channels of the two-pore domain potassium (K2P) family contain two pore domains rather than one and an unusually long pre-pore extracellular linker called the M1P1 loop. The TASK (TASK1, TASK3, and TASK5) subfamily of K2P channels is regulated by a number of different pharmacological and physiological mediators. At pH 7.4 TASK3 channels are selectively blocked by zinc in a manner that is both pH_o- and $[K]_o$-dependent. Mutation of both the Glu-70 residue in the M1P1 loop and the His-98 residue in the pore region abolished block, suggesting the two residues may contribute to a zinc binding site. Mutation of one Glu-70 residue and one His-98 residue to cysteine in TASK3 fixed concatamer channels gave currents that were enhanced by dithiothreitol and then potently blocked by cadmium, suggesting that spontaneous disulfide bridges could be formed between these two residues. Swapping the M1P1 loops of TASK1 and TASK3 channels showed that the M1P1 loop is also involved in channel regulation by pH. Therefore, the TASK3 M1P1 loop lies close to the pore, regulating TASK3 channel activity.

Background, or leak, potassium currents play an important role in the regulation of the resting membrane potential and excitability of mammalian neurons. The two-pore domain potassium (K2P) channel family is open across the physiological voltage range and is believed to underlie many of these leak currents (1–5). So named as each α-subunit of K2P channels contains two pore domains, or P-domains, the channels also contain an unusually large extracellular pre-pore linker called the M1P1 loop. This linker is believed to form a self-interacting domain that is essential for channel dimerization (6) and may play a role in channel regulation (7–9).

There are currently 15 members of this family, which can be divided into six subfamilies on the basis of structural and functional properties (4, 10, 11). Among these subfamilies is the TWIK-related acid-sensitivepotassium subfamily (TASK1 (K_{2P} 3.1), TASK3 (K_{2P}9.1), and TASK5 (K_{2P} 15.1)). TASK1 and TASK3 K2P channels are regulated by a wide variety of chemical stimuli (12, 13) and are responsible for leak potassium currents in many neurons, including cerebellar granule neurons (*e.g.* 14–20).

TASK channels are sensitive to extracellular acidification, with a histidine at position 98 shown to be crucial for the pH sensitivity of TASK1 and TASK3 channels (7, 21–23), although the mechanism behind TASK1 pH sensitivity is not yet fully understood as mutation of this histidine in TASK1 merely shifts pH sensitivity rather than abolishes it (7). We have shown previously that zinc is a selective blocker of TASK3 channels with little effect on TASK1 in physiological conditions (24). This selective block involves both His-98 and a glutamate residue (Glu-70) within the M1P1 loop, suggesting that the M1P1 loop plays an important role in channel regulation (24). Indeed, Glu-70 on the M1P1 loop is also essential for the block of TASK3 current by ruthenium red (25) and other divalent cations (26).

The long extracellular M1P1 loop is not conserved in potassium channels with known crystal structures. However, a structural homology model of TASK1 based on known potassium channel structures shows the M1P1 loops lying in close association at position Asn-53 (27), a position homologous to TWIK1 C69, an M1P1 loop cysteine residue responsible for channel dimerization (6).

Two cysteines may form a disulfide bond if they are close to each other (β-carbon distance = 4–5 Å) (28), and therefore the engineered disulfide approach, involving introduction of cysteine residues and looking for disulfide bond formation, is a useful tool that has been widely used to determine regions of close proximity for a number of membrane proteins, including potassium channels (29).

In this study we describe in more detail the mechanism of TASK3 zinc block. We confirm that the zinc block involves a glutamate residue in the M1P1 loop and His-98 in the pore region, and we demonstrate that engineered cysteines at positions 70 and 98 are able to form both inter- and intrasubunit spontaneous disulfide bonds. The M1P1 loops of TASK3 channels therefore lie in close apposition to the pore, and through exchange of the M1P1 loops between TASK3 and TASK1 channels we demonstrate that this unusual linker plays a role in the TASK channel pH-sensing mechanism.

EXPERIMENTAL PROCEDURES

Mutations and Truncations—Point mutations were introduced by site-directed mutagenesis into the TASK3 channel

* This work was supported in part by the Medical Research Council and the Australian Research Council (ARC). The costs of publication of this article were defrayed in part by the payment of page charges. This article must therefore be hereby marked "*advertisement*" in accordance with 18 U.S.C. Section 1734 solely to indicate this fact.

[1] Both authors contributed equally to this work.
[2] An ARC postdoctoral fellow.
[3] To whom correspondence should be addressed. Fax: 44-1634-883927; E-mail: a.a.mathie@kent.ac.uk.

clones using the QuikChange kit (Stratagene). A pair of short (25–35 bases) complementary oligonucleotide primers incorporating the intended mutation were synthesized (MWG-Biotech, Ebersberg, Germany). TASK3 concatamer channels were created with a 6-amino acid linker between the two subunits. In each case, point mutations were made to individual subunits before the final concatamers were formed. Chimeric TASK channels were constructed by swapping M1P1 loops between family members. This was achieved by the introduction of silent mutations to create unique restriction sites, Xho1 and BamH1, either side of the M1P1 region using standard PCR techniques described above. Chimeras were then formed by "cutting and pasting" of this region between the TASK family members. For TASK2 channels a non-silent BamH1 restriction site was created for cutting and pasting and further point mutations undertaken to remove the non-silent mutations. Mutant DNA and chimeric constructs were sequenced (MWG-Biotech, UK/SUPAMAC, Sydney) to confirm the introduction of the correct mutated bases.

tsA-201 Cell Culture Preparation—Modified human embryonic kidney 293 cells (tsA-201) were maintained in 5% CO_2 in a humidified incubator at 37 °C in growth medium (89% Dulbecco's modified Eagle's medium, 10% heat-inactivated fetal bovine serum, 1% penicillin (10,000 units ml^{-1}) and streptomycin (10 mg ml^{-1}). When the cells were 80% confluent, they were split and plated for transfection onto glass coverslips coated with poly-D-lysine (1 mg ml^{-1}) to ensure good cell adhesion. The cells were transiently transfected using the calcium phosphate method. 0.3–1 μg of cDNA expression vector encoding a mouse or human TASK3 subunit was added to each 15-mm well, and 0.3–1 μg of a plasmid encoding the cDNA of green fluorescent protein was included to identify cells expressing K2P channels. Following an 18–24-h incubation period at 3% CO_2 the cells were rinsed with saline and fresh growth medium was added to the wells. The cells were incubated at 37 °C with 5% CO_2 for 24–60 h before electrophysiological measurements were made.

Electrophysiological Recordings from tsA-201 Cells—Whole cell voltage clamp recordings were made from tsA-201 cells transiently transfected with hTASK3 or hTASK1 wild type or mutated channels. The composition of the control extracellular solution was (in mM) 145 NaCl, 2.5 KCl, 3 $MgCl_2$, 1 $CaCl_2$, 10 HEPES, (titrated to pH 7.4 with NaOH). Glass microelectrodes were pulled from thick-walled borosilicate glass capillaries. Fire-polished pipettes were backfilled with 0.2 μm filtered intracellular solution (composition in mM: 150 KCl, 3 $MgCl_2$, 5 EGTA, 10 HEPES (titrated to pH 7.4 with KOH)). Cells were voltage-clamped using an Axopatch 1D amplifier (Molecular Devices, Sunnyvale, CA) and low pass-filtered at 5 kHz before sampling (2–10 kHz) and online capture. Data acquisition was carried out using pClamp software (Molecular Devices). tsA-201 cells were held at −80 mV and then subjected to a step to −40 mV for 500 ms, followed by a 500- or 1000-ms voltage ramp from −110 to +20 mV (or similar voltage ranges) once every 5 s. All electrophysiological measurements were carried out at room temperature (21–23 °C). Modulatory compounds were applied by bath perfusion at a rate of 4–5 ml min^{-1}. Complete exchange of bath solution occurred within 100–120 s.

Two-electrode Voltage Clamp Recording—Xenopus laevis oocytes were prepared exactly as described previously (30). All experiments were approved by the Animal Ethics Committee of the University of Sydney. Recordings were made using the two-electrode voltage clamp technique. Oocytes were placed in a recording chamber 1–3 days after injection of cDNA encoding either hTASK1, hTASK2, hTASK3, or mutant or chimeric channels and continuously perfused with ND96 at room temperature (21–23 °C). Tris or MES[4] buffer replaced HEPES for solutions above 8 and below 7, respectively. $ZnCl_2$ was kept as a 10-mM stock and diluted as required. Microelectrodes were pulled to tip resistances of 0.5–1.5 MΩ. Uninjected oocytes were used as control. Currents present in uninjected oocytes were so small (maximum 0.5 μA at +60 mV) compared with those in injected oocytes that no compensation was deemed necessary. Standard test ramps were run from a holding potential of −90 mV. Oocytes were stepped to +30 mV for 50 ms, and then a ramp of 450-ms duration, from −120 to +60 mV, was run with the initial step to −120 mV being held for 50 ms to ensure capacity currents had returned to base line. Current responses, digitized at 2 kHz and filtered at 1 kHz using a Geneclamp 500B (Molecular Devices), were recorded and analyzed using pClamp9 software (Molecular Devices), Excel 2003, (Microsoft Corp., Seattle, WA), and Prism 4 (GraphPad Software Inc., San Diego, CA).

Data Analysis—Data were analyzed using Clampfit software (Axon Instruments), Excel (Microsoft Corp.), and Origin (Microcal). Individual experimental pH data were fitted with sigmoidal dose-response curves. Statistical comparisons were carried out using Student's *t* test or one-way analysis of variance, and *p* values <0.05 were regarded as significant. Results are given as means ± S.E. of the mean with *n* as the number of experiments.

Drugs, Chemicals, and cDNA—Cadmium chloride, ruthenium red, and dithiothreitol (DTT) were obtained from Sigma. Apart from DTT, compounds were made up in either DMSO or water and diluted in external solution prior to experimentation. DTT was added directly to the external solution from solid (to give appropriate final concentrations) immediately prior to recording. The human TASK3, TASK2, and TASK1 K2P channel clones in the pcDNA 3.1 vector were from Dr. Helen Meadows (GlaxoSmithKline).

RESULTS

Zinc Is a Relatively Selective Blocker of TASK3 Channels Compared with TASK1 Channels—In control solutions (pH_o 7.4, $[K]_o$ 2.5 mM), zinc (100 μM) substantially inhibited TASK3 currents by 87 ± 2% (mean ± S.E., $n = 12$) but inhibited TASK1 currents by only 11 ± 4% ($n = 8$) (see Fig. 1, *A* and *B*, also Refs. 19, 24). Mutation of the histidine residue adjacent to the selectivity filter in the first pore domain of TASK3 (H98A) reduced the effect of zinc on TASK3 chan-

[4] The abbreviations used are: MES, 4-morpholineethanesulfonic acid; DTT, dithiothreitol; WT, wild type.

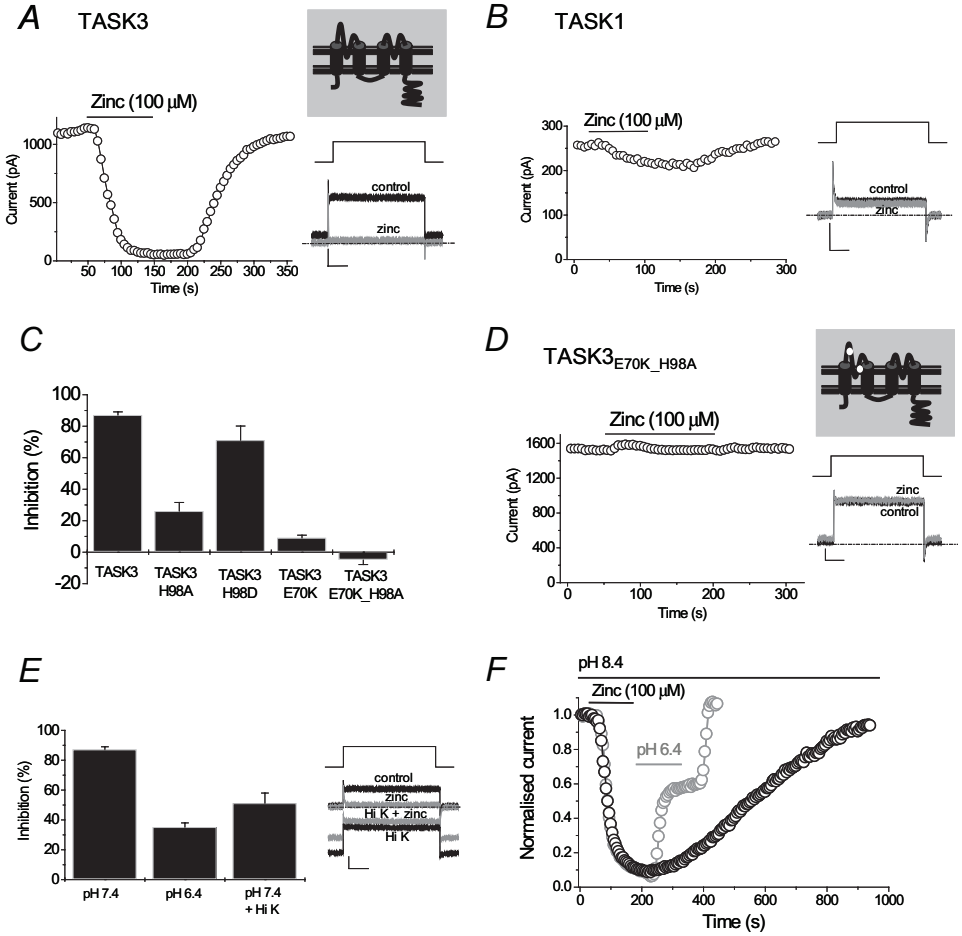

FIGURE 1. **Glu-70 and His-98 are critical residues on TASK3 channels for block by zinc.** Time course plots showing block by zinc (100 μM) of TASK3 at pH 7.4 (*A*) and TASK1 at pH 7.4 (*B*). A schematic representation of TASK3 is shown in *A*. *C*, histogram showing block of WT TASK3 and various mutated TASK3 channels by zinc (100 μM). *D*, representative time course plot showing lack of effect of zinc (100 μM) on $TASK3_{E70K,H98A}$ channel currents. The mutations are shown as *white dots* on the TASK3 channel construct schematic. *E*, histogram showing effect of pH and high extracellular potassium (100 mM) on modulation of TASK3 channel currents by zinc. *F*, rate of recovery of block of TASK3 channel currents by zinc is greatly speeded up by extracellular acidification. Note that, in the case of pH 6.4, hydrogen ions also block the channel, which explains the "N" shape for the recovery of the current. Representative traces are shown as *insets* (*A*, *B*, *D*, and *E*) with voltage steps from −80 to −40 mV and then back to −80 mV and calibration bars of 500 pA and 200 ms in each case. *Error bars* in *C* and *E* are S.E. of the mean.

nels (Fig. 1*C*) (24). However, in contrast to $TASK3_{H98A}$, $TASK3_{H98D}$ channels (where the histidine was replaced by the aspartate seen most commonly in potassium channels) were still substantially blocked by zinc. Thus, an additional region of the channel must influence zinc block to account for both the differential zinc sensitivity of TASK3 and TASK1 channels and the zinc sensitivity of $TASK3_{H98D}$ channels. Mutating a glutamate residue in the M1P1 loop of TASK3 to the lysine found in TASK1 ($TASK3_{E70K}$) also reduced the effect of zinc (Fig. 1*C*) while the double mutation (E70K,H98A) abolished the effect of zinc on TASK3 channels (Fig. 1, *C* and *D*).

Zinc Block of TASK3 Channels Depends on pH_o and $[K]_o$—The commonality in an identified site of action of pH (see Ref. 22) and zinc (namely the His at position 98) suggests that these two compounds may interact when both are present. This was, indeed, found to be the case. While zinc was a potent, selective blocker of TASK3 at pH 7.4, acidic pH could, at least in part, overcome the effects of zinc. At pH 6.4, TASK3 currents were blocked significantly less by 100 μM zinc (35 ± 3%, $n = 4$) compared with pH 7.4 (Fig. 1*E*). Similarly, zinc became a significantly more effective blocker of TASK1 channels when pH_o was raised to 8.4 (inhibition of 55 ± 4%, $n = 8$).

The interaction between zinc and hydrogen ions could also be demonstrated by considering recovery of current amplitude following block by zinc. In the example shown, TASK3 currents were potently blocked at pH 8.4 by 100 μM zinc (Fig. 1*F*). Full recovery from block took a considerable time (~700 s for the example shown); however, this recovery was much faster (>3-fold faster in this cell) if the channels were exposed briefly to pH 6.4 external solution during wash out of zinc. Because mutation of histidine at position 98 interferes with both zinc and hydrogen ion block, the most parsimonious explanation for these data is that zinc and hydrogen ions compete for an overlapping binding site.

Hydrogen ions are less effective blockers of TASK channels in the presence of high extracellular [K] (31), so it was of interest to determine whether changing the extracellular [K] also interfered with block by zinc of TASK3 channels. Fig. 1*E* shows the effect of 100 μM zinc on TASK3 channels at pH 7.4 in normal solution and in the presence of high (100 mM) $[K]_o$. Zinc was significantly less effective at blocking current in high $[K]_o$ compared with control.

To demonstrate further the individual importance of both His-98 and residues in the M1P1 loop in zinc block, we utilized TASK2 ($K_{2P}5.1$) channels. Although named TASK2, these channels share greater amino acid homology with the alkaline-sensitive TALK channels (10). TASK2 channels do not contain a homologous histidine within the first pore region and are insensitive to zinc (24). Introducing a histidine at a homologous site to TASK3 His-98 in TASK2 ($TASK2_{N103H}$) did not lead to zinc-sensitive currents (Fig. 2, *A*, *B*, *E*, *F*). Expression of a chimera consisting of the body of TASK2 with the M1P1 loop of TASK3 ($TASK2_{TASK3M1P1}$) in *Xenopus* oocytes also led to zinc-insensitive currents (Fig. 2, *C* and *E*). However, the presence of both the TASK3 M1P1 loop and the pore-residing histidine ($TASK2_{TASK3M1P1\_N103H}$) enabled zinc block at pH 7.4, with a 51 ± 5% ($n = 5$) inhibition seen at 100 μM zinc, close to the zinc

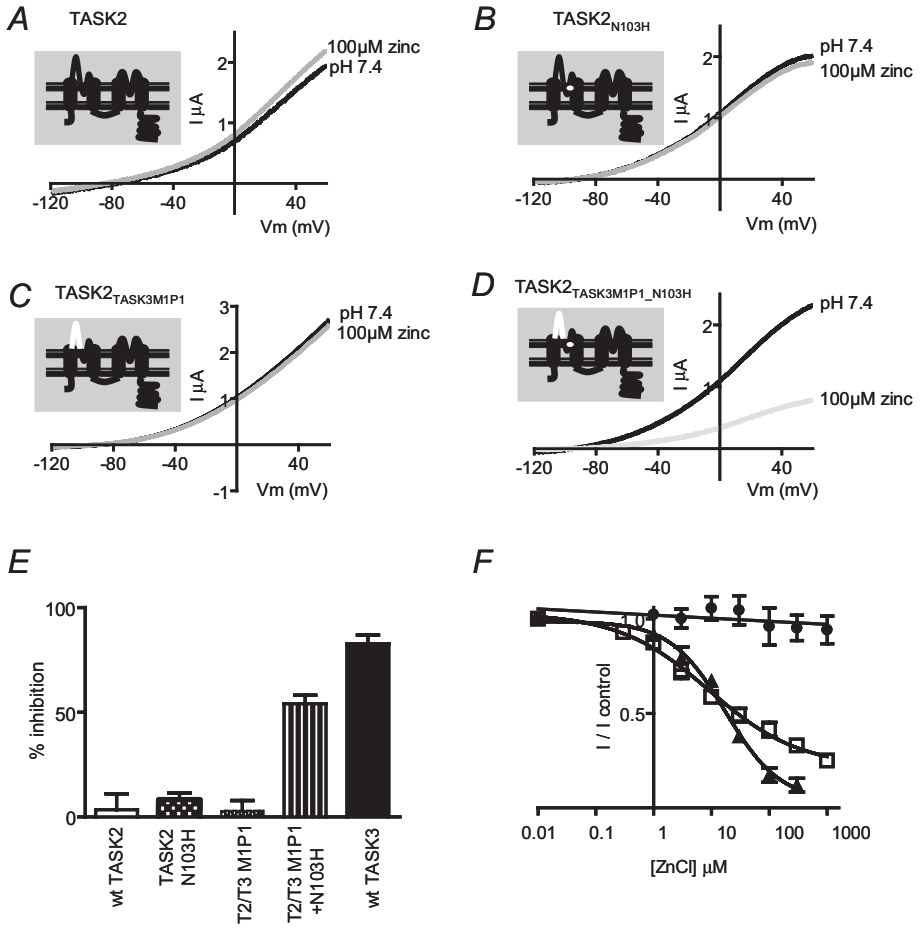

FIGURE 2. **The M1P1 loop of TASK3 and a histidine at position 103 confer zinc sensitivity to TASK2 channels.** *A–D*, current-voltage relationships showing the effect of zinc (100 μM) on WT TASK2 channels (*A*), $TASK2_{N103H}$ channels (*B*), $TASK2_{TASK3M1P1}$ chimeric channels (*C*), and $TASK2_{TASK3M1P1\_N103H}$ chimeric channels (*D*). In each panel (*A–D*) a schematic of the TASK2 channel construct is shown. Mutations and chimeric alterations are shown in *white*. *E*, histogram showing block of WT and mutated TASK2 channels by zinc (100 μM). *F*, concentration response curves for zinc block of TASK3 channels and mutated TASK2 channels. The *filled triangles* are TASK3, the *filled circles* are $TASK2_{TASK3M1P1}$, and the *open squares* are $TASK2_{TASK3M1P1\_N103H}$. *Error bars* in *E* and *F* are S.E. of the mean.

sensitivity of TASK3 channels (Fig. 2, *A*, *D–F*). Thus, the block of TASK3 channels by zinc is only recapitulated in TASK2 channels when both the M1P1 loop and the pore histidine residue from TASK3 are present.

The Effect of DTT on TASK3 Channel Cysteine Mutations—The importance of both Glu-70 and His-98 in block by zinc suggests that these amino acids may be located close to each other in the channel to form a binding site for zinc (see also Ref. 24). Mutation of both Glu-70 and His-98 to Cys gave channels that were virtually non-functional (2 ± 1 pA/pF, n = 14); however, current was partially restored when cells were treated with the reducing agent DTT (5 mM), which breaks disulfide bonds (18 ± 3 pA/pF, n = 16, Fig. 3*A*). Zinc was a potent blocker of these channels following application of DTT with 100 μM, giving 89 ± 3% inhibition (n = 5). Cysteine residues are very common in metal binding motifs such as zinc fingers in proteins and often contribute to the modulatory binding sites for zinc on ion channels (see Ref. 32). While E70C mutated channels alone gave functional currents that were unaffected by DTT, carrying out the same experiment with only His-98 modified to a cysteine residue gave broadly similar results to that with the $TASK3_{E70C,H98C}$ double mutation. Current in $TASK3_{H98C}$ channels was 6 ± 1 pA/pF (n = 15), and this was restored to 62 ± 10 pA/pF (n = 10) following DTT (Fig. 3*B*). Again, zinc was a potent blocker of the restored current (88 ± 4% inhibition, n = 4). Indeed, inhibition was difficult to reverse unless DTT was reapplied to the cells. Reversal by DTT is most likely due to the ability of this compound to powerfully chelate zinc (33). Thus, our results with cysteine mutations and DTT show that the two mutated histidine residues form a disulfide bond in the $TASK3_{H98C}$ channel dimer but do not provide evidence as to whether the Glu-70 residues are close enough to the His-98 residues to form bonds when also mutated to cysteine residues.

Sensitivity of TASK3 Tandem Channel Constructs to DTT and Cadmium—To be able to address these interactions further, we needed to construct tandem channel constructs that would allow us to mutate a residue on only one or the other of the subunits that make up the functional channel dimer. Our initial construct was to join two wild type (WT) TASK3 channels in a forced concatamer. This construct gave functional channels that were inhibited as predicted by zinc (100 μM, 90 ± 1%, n = 3, Fig. 3*C*) and ruthenium red (10 μM, 68 ± 3%, n = 5), another selective blocker of TASK3 channels (25).

Mutation of a single His-98 residue to Cys (on the second subunit of the tandem construct, TASK3/$TASK3_{H98C}$) gave functional currents, and these were now no longer enhanced by perfusion of DTT (4 ± 3% inhibition, n = 4, Fig. 3*D*), in contrast to the $TASK3_{H98C}$/$TASK3_{H98C}$ channel dimer above. This shows that the cysteine residue that we have introduced at position 98 is only capable of forming a spontaneous disulfide bond with another introduced cysteine residue and not with any cysteine residues present in the WT TASK3 channel.

The amplitude of current through constructs where one Glu-70 residue and one His-98 residue were mutated to cysteine on one or the other of the two subunits of the tandem construct was significantly enhanced by DTT treatment (Fig. 3, *E* and *F*). Currents through the $TASK3_{E70C,H98C}$/TASK3 construct were enhanced by 43 ± 9% (n = 6) whereas DTT enhanced currents through the $TASK3_{E70C}$/$TASK3_{H98C}$ construct by 39 ± 7% (n = 12), the latter construct consisting of channels with one mutation in each subunit.

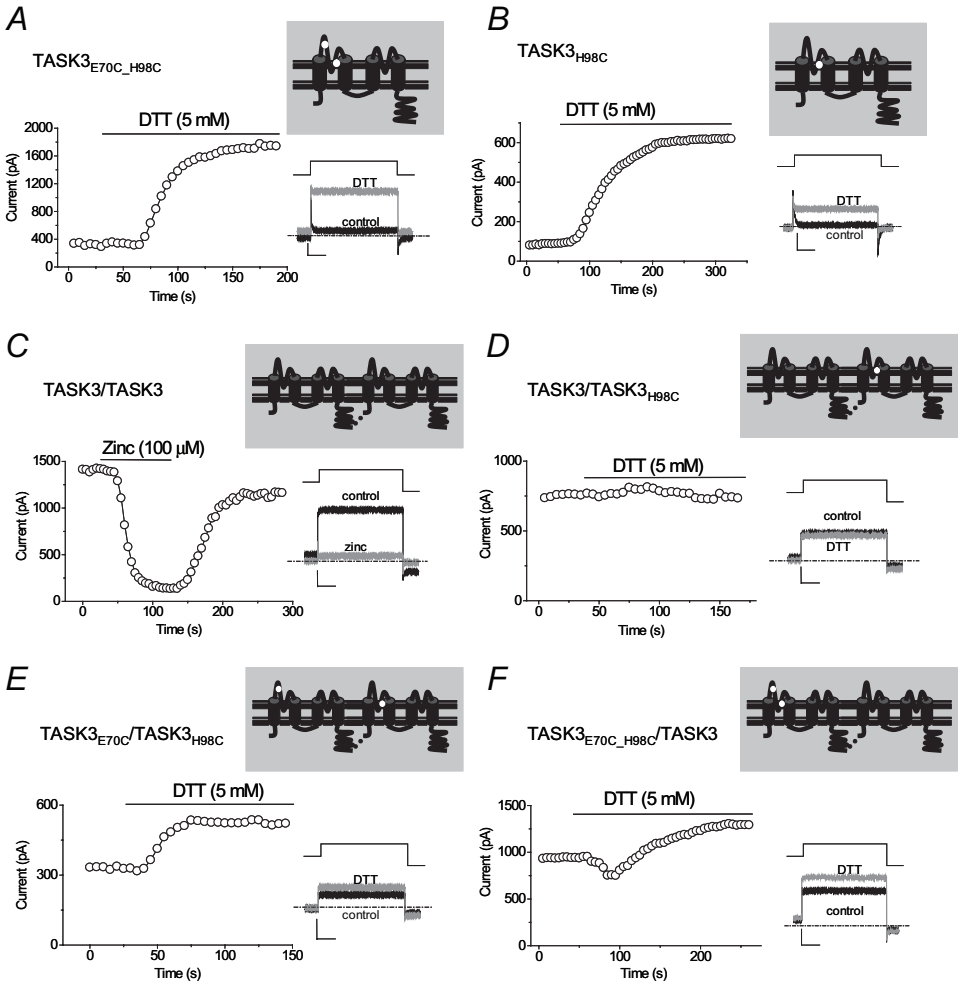

FIGURE 3. **TASK3 cysteine mutant channels are enhanced by DTT.** *A* and *B*, time course plots showing that $TASK3_{E70C,H98C}$ (*A*) and $TASK3_{H98C}$ (*B*) channels have small base-line currents but that these are dramatically enhanced by application of DTT (5 mM). *C*, time course plots showing that TASK3/TASK3 concatamer channels function normally and are blocked by zinc (100 μM). *D–F*, time course plots showing that TASK3/$TASK3_{H98C}$ concatamer channels (*D*) are insensitive to DTT (5 mM) but that $TASK3_{E70C}$/$TASK3_{H98C}$ (*E*) and $TASK3_{E70C,H98C}$/TASK3 (*F*) concatamer channels are enhanced by DTT (5 mM). Representative traces are shown as *insets* (*A–F*) with voltage steps from −80 to −40 mV and then back to −80 mV in *A* and *B* and back to −110 mV in *C–F*. Calibration bars are 500 pA and 200 ms in each case. For each panel, a schematic of the channel construct is shown with mutations illustrated as *white dots*.

Our data therefore suggest that some degree of cross-linking can occur, spontaneously, between the Cys-70 and Cys-98 residues in these mutants, even when the cysteine residues are on different subunits of the dimer. The M1P1 loop therefore must lie close to the pore. Because the enhancement by DTT is similar in magnitude whether the cysteine residues at positions Cys-70 and Cys-98 are on the same subunit or opposite subunits, this suggests that inter- and intrasubunit interactions are equally strong. To test this idea further, we used cadmium ions that can bind strongly to two closely apposed cysteine residues (*e.g.* Ref. 34). Cadmium (at 10 μM) had no significant effect on WT TASK3 channels (2 ± 2% inhibition, $n = 4$, Fig. 4*A*); however, it caused a small, reversible inhibition of the mutated concatamers (Fig. 4, *B–D*). For the $TASK3_{E70C,H98C}$/TASK3 construct, cadmium produced a 13 ± 6% inhibition ($n = 4$) whereas the $TASK3_{E70C}$/$TASK3_{H98C}$ construct was inhibited by 18 ± 2% ($n = 10$). This is comparable with the block seen for the single mutant concatamer channel (TASK3/$TASK3_{H98C}$) that was blocked by 10 μM cadmium by 25 ± 3% ($n = 6$) before DTT and 27 ± 2% ($n = 6$) following DTT and suggests reversible cadmium binding to single free cysteine residues (see also Ref. 34). Following treatment with DTT, cadmium was significantly ($p < 0.05$) more effective at blocking current through these concatamer channels (Fig. 4, *B* and *C*). The $TASK3_{E70C,H98C}$/TASK3 construct was inhibited by cadmium (10 μM) by 57 ± 5% ($n = 5$) after DTT, whereas the $TASK3_{E70C}$/$TASK3_{H98C}$ construct was inhibited by 63 ± 4% ($n = 3$). Furthermore, following DTT treatment, block by cadmium was difficult to reverse unless DTT was reapplied to the cells (Fig. 4, *B* and *D*), again supporting the hypothesis that these residues are in close apposition.

The $TASK3_{N53C}$ Channel Construct Is Insensitive to DTT and Cadmium—In contrast to this, M1P1 residues that have previously been assumed to be closely associated in TASK1 (35) that are also conserved in TASK3 may not, in fact, be in close apposition. We created a $TASK3_{N53C}$ mutant and looked for evidence of disulfide bridge formation. Expression of the mutant in *Xenopus* oocytes gave currents that were WT-like (8.5 ± 2 μA ($n = 8$) and 7.0 ± 1 μA ($n = 13$) for mutant and WT TASK3 channels, respectively). Full pH response curves showed no change in pH sensitivity of the mutant channel with a pK_a of 6.4 ± 0.1 ($n = 4$), compared with a pK_a = 6.6 ± 0.03 ($n = 13$) for WT TASK3 (Fig. 4*E*). Application of 5 mM DTT or 10 μM cadmium had no significant effect on current size at 30 mV, with a 6.9 ± 4% ($n = 8$) increase and a 3.7 ± 1% ($n = 5$) decrease in current recorded, respectively. A similar lack of effect of DTT and cadmium on this mutant was seen when these channels were expressed in tsA-201 cells (Fig. 4*F*).

The M1P1 Loop Influences the pH Sensitivity of TASK1 Channels—TASK1 channels are more sensitive to extracellular pH than TASK3 (7, 21–23). The close proximity of residues on the M1P1 loop to the apparent pH sensor in TASK3 suggests that the M1P1 loop could play a role in determining the pK_a of channel conductance. To test this hypothesis we generated chimeric channels in which the M1P1 loop was swapped between TASK1 and TASK3 and visa versa.

Expression of the chimeras formed from TASK1 with the TASK3 M1P1 loop ($TASK1_{TASK3M1P1}$) and TASK3 with the TASK1 M1P1 loop ($TASK3_{TASK1M1P1}$) in *Xenopus* oocytes

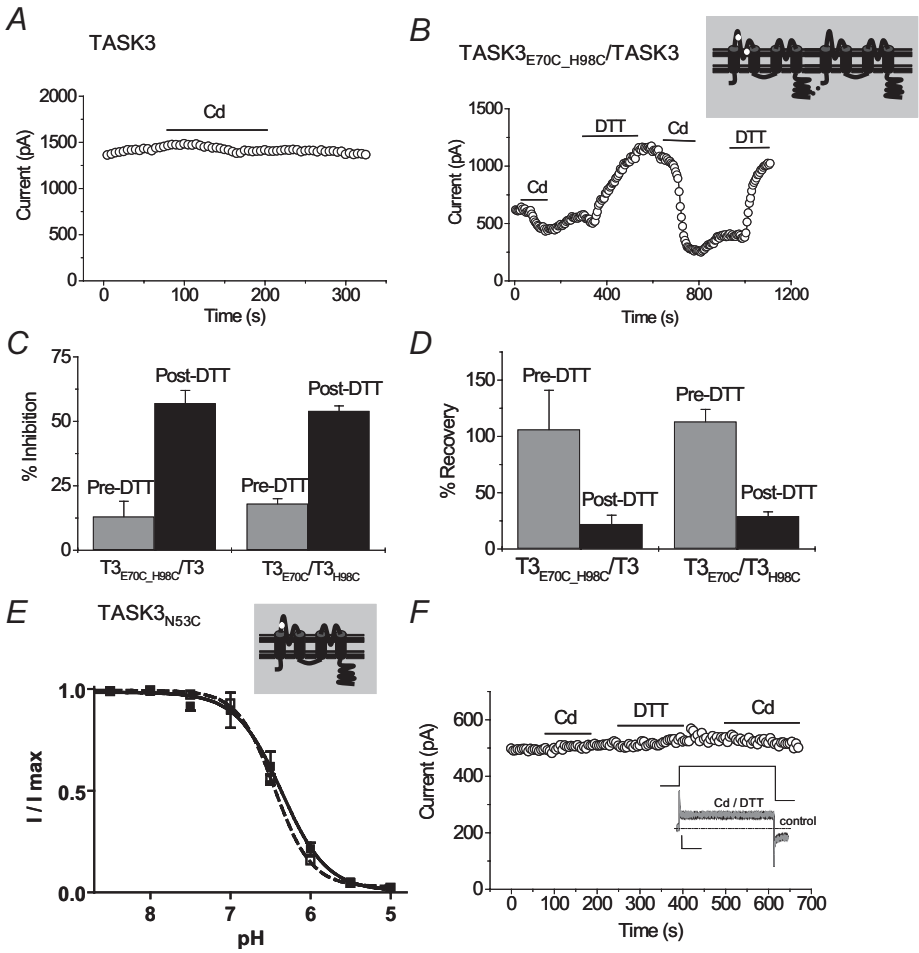

FIGURE 4. **TASK3 cysteine mutant, concatamer channels are inhibited by cadmium.** *A* and *B*, time course plots showing that TASK3 channels (*A*) are unaffected by cadmium (10 μM) whereas $TASK3_{E70C,H98C}$/TASK3 concatamer channels (*B*) are blocked by cadmium (10 μM) and that this block is substantially enhanced and difficult to reverse following DTT (5 mM). *C*, histogram showing that $TASK3_{E70C}$/$TASK3_{H98C}$ and $TASK3_{E70C,H98C}$/TASK3 concatamer channels are blocked by cadmium (10 μM) and that this block is enhanced following DTT (5 mM). *D*, histogram showing that block of $TASK3_{E70C}$/$TASK3_{H98C}$ and $TASK3_{E70C,H98C}$/TASK3 concatamer channels by cadmium (10 μM) is fully reversible under normal conditions but poorly reversible following DTT (5 mM). $TASK3_{N53C}$ mutant channels have an unaltered pH sensitivity (*E*) and are unaffected by DTT (5 mM) or cadmium (10 μM) (*F*), the latter either before or after DTT treatment. Representative traces are shown as an *inset* (*F*) with voltage steps from −80 to −40 mV and then back to −110 mV and calibration bars of 500 pA and 200 ms. In *B* and *E*, a schematic of the channel construct is shown with mutations illustrated as *white dots*. *Error bars* in *C* and *D* are S.E. of the mean.

gave functional currents that were still potassium-selective. Similarly to WT TASK channels, the chimeras were sensitive to extracellular pH changes (Fig. 5, *A–D*). Full pH response curves (Fig. 5*E*) showed a pK_a for inhibition of $TASK3_{TASK1M1P1}$ that was significantly shifted by 0.3 of a pH unit compared with WT TASK3 ($TASK3_{TASK1M1P1}$, $pK_a = 6.7 \pm 0.02$ ($n = 11$), TASK3 $pK_a = 6.4 \pm 0.09$ ($n = 10$), $p < 0.005$). The pK_a of the $TASK1_{TASK3M1P1}$ was significantly shifted by 0.5 of a pH unit compared with WT TASK1 ($TASK1_{TASK3M1P1}$, $pK_a = 7.0 \pm 0.06$, ($n = 15$), TASK1, $pK_a = 7.5 \pm 0.03$ ($n = 11$), $p < 0.005$). Furthermore, zinc sensitivity could be imparted to TASK1 channels by inserting the TASK3 M1P1 loop, and, conversely, zinc sensitivity was lost in TASK3 channels when the M1P1 loop was replaced with that from TASK1 (Fig. 5*F*). Overall, these data demonstrate that the M1P1 loop can regulate TASK channel function by influencing sensitivity to both zinc and pH.

DISCUSSION

Zinc Block of TASK3 Channels—We have shown that zinc block of TASK3 channels depends on both $[pH]_o$ and $[K]_o$, with zinc being less effective in acidic pH or high extracellular potassium. Thus, zinc is a clear discriminator between TASK3 and TASK1 channels only under physiological recording conditions. The interaction between zinc and hydrogen ion block of TASK channels may suggest that these ions compete for an overlapping binding site on the channel. This idea is supported by the observation that, as seen for zinc ions in this study, hydrogen ions are less effective blockers of TASK channels in the presence of high extracellular $[K]_o$ (31). Indeed, an identified amino acid, His-98, is involved in both zinc block (24) and in the pH-sensing mechanism of TASK3 channels (22, 23). Although we cannot completely rule out the possibility that it is the reduction of $[Na]_o$ rather than the increase in $[K]_o$ that modifies zinc and pH sensitivity, we think it more likely that the increase in $[K]_o$ is responsible (see also Ref. 31) because replacement of $[Na]_o$ with choline or *N*-methyl-D-glucamine, although reducing current amplitude considerably, does not alter the sensitivity of TASK3 channels to changes in pH.[5]

In terms of the mechanism of zinc block of TASK channels, our original explanation of the results we obtained (24) was that zinc was at its most potent when a four-coordinate binding site (of 2 × Glu-70 and 2 × His-98) is present, such as in the TASK3 WT homodimer channel, because the action of zinc was reduced either when His-98 or Glu-70 was mutated or, in this study, when His-98 was protonated. These findings are supported by our additional data showing that a TASK3/TASK1 chimera ($TASK3_{TASK1M1P1}$) was also not sensitive to zinc and, importantly, that TASK2 channels can acquire zinc sensitivity only when both the TASK3 M1P1 loop and His-103 are present ($TASK2_{TASK3M1P1\_N103H}$).

Glu-70 in the M1P1 Loop Is Closely Apposed to His-98 in the Pore Region—Because Glu-70 and His-98 are suggested to form a binding site for zinc, this implies that these amino acids are located close to each other in the tertiary TASK3 channel structure. Our cysteine mutation studies and experiments on

[5] L. J. Evans, E. L. Veale, and A. Mathie, unpublished observations.

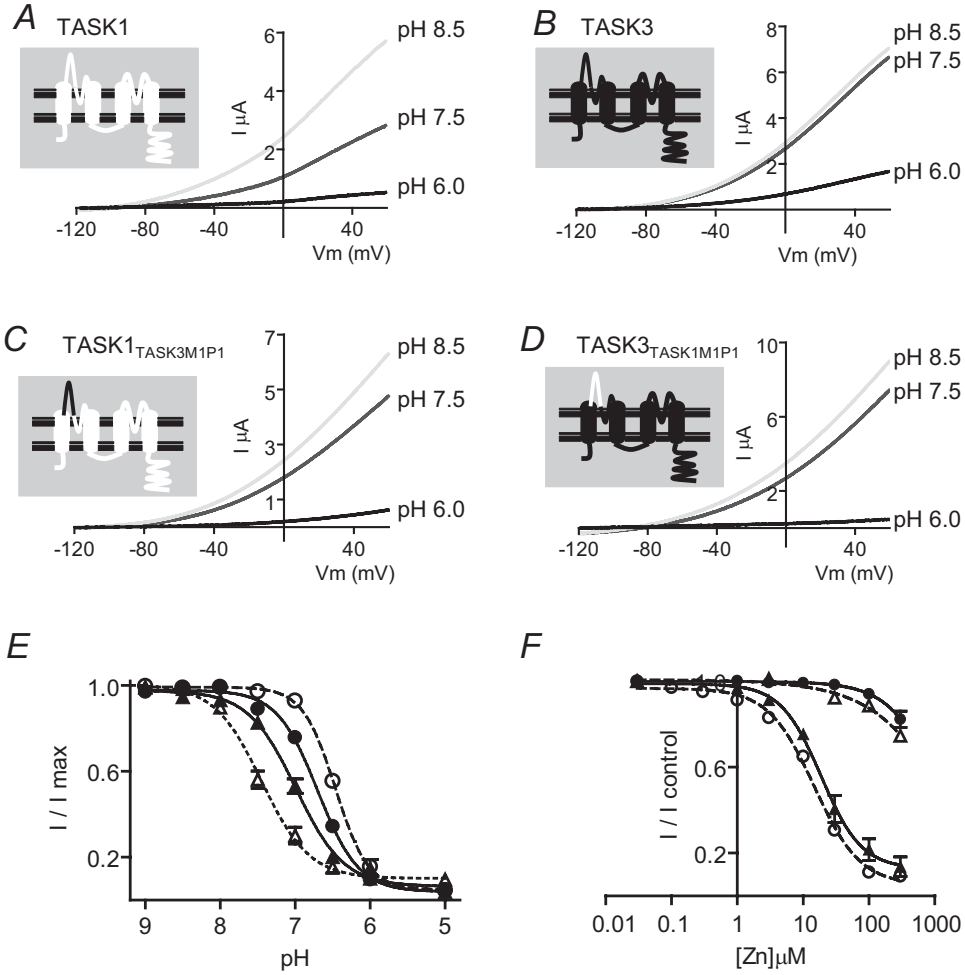

FIGURE 5. **The M1P1 loop influences the pH sensitivity of TASK1 and TASK3.** Example currents demonstrate pH sensitivity in oocytes expressing WT TASK1 (*A*), WT TASK3 (*B*), $TASK1_{TASK3M1P1}$ chimera (*C*), and $TASK3_{TASK1M1P1}$ chimera (*D*), respectively. In each panel (*A–D*), a schematic of the chimeric channel construct is shown with TASK1 components in *white* and TASK3 in *black*. *E*, full pH response curves showed a pK_a for inhibition of $TASK3_{TASK1M1P1}$ (*closed circle*) that was slightly but significantly shifted compared with WT TASK3 (*dashed line*, *open circle*). The pK_a of the $TASK1_{TASK3M1P1}$ chimera (*closed triangle*) was also significantly shifted by 0.5 of a pH unit compared with WT TASK1 (*dashed line*, *open triangle*). *F*, zinc concentration response curves demonstrate that WT TASK1 (*dashed line*, *open triangle*) and $TASK3_{TASK1M1P1}$ (*closed circle*) are essentially zinc-insensitive, whereas the zinc sensitivity of the $TASK1_{TASK3M1P1}$ chimera (*closed triangle*) overlies that of WT TASK3 (*dashed line*, *open circle*).

TASK3 channel concatamers add support to this suggestion. A significant enhancement of current through mutated TASK3 channel concatamers by DTT was observed, whether the E70C and H98C are on the same subunit in the concatamer or on opposite subunits, whereas a concatamer with only H98C on the second subunit was unaffected by DTT.

Cadmium can bind strongly to two closely apposed cysteine residues to form long-lasting bonds, providing they are separated by 5 Å or less (34). At a concentration that had no effect on WT TASK3 channels, we observed a small block of mutated TASK3 channel concatamers, suggesting that some reversible binding to free, introduced cysteine residues occurs. However, following treatment of the cells with DTT, cadmium became a powerful blocker of the mutated concatamers with an effect that was hard to reverse unless we re-applied DTT. This suggests that the disulfide bonds broken by DTT release closely apposed cysteine residues that were now available to bind strongly to cadmium ions and alter channel conformation to block current flow. Taken together, these data provide strong evidence that Glu-70 and His-98 are in close apposition (within 4–5 Å of each other) (28, 34) in TASK3 channels.

A recent structural homology model of TASK1 (27) proposed that the M1P1 loops are forced in close association at position Asn-53, a position homologous to the TWIK1 M1P1 cysteine responsible for channel dimerization (6). In this study, TASK3 N53C mutant channels were no different to wild type both in terms of current size and pH sensitivity. While our data do not rule out the possibility that these amino acids are in close apposition and that disulfide bonds may be still be formed between the M1P1 loops at this position, if they do occur these must either be inaccessible or simply do not affect channel function, because application of DTT or cadmium had no effect on currents through the channel.

The pH-sensing Mechanism of TASK Channels—His-98 acts as the pH sensor of both TASK3 and TASK1 channels (7, 21–23). However, although mutation of His-98 abolishes TASK3 pH sensitivity, it only reduces the pH sensitivity of TASK1, implying an additional pH-sensing mechanism in TASK1 channels (7, 23). An aspartate (Asp-204) within the second pore region optimizes pH sensitivity in TASK1 (35). However, this aspartate is conserved throughout the entire K2P family, and it may be that it serves an important role in structuring the selectivity pathway rather than being a pH sensor *per se*. Indeed, recent data from Yuill *et al.* (27) show that mutations throughout the pore region of TASK1 that affect the selectivity of the channel also affect the pH sensitivity.

Intriguingly, the recently discovered *Drosophila* TASK channels, named dTASK6 and dTASK7, have pH sensitivity that is independent of His-98 (9). In these channels a region including the first 20 of the 48 amino acids that form the M1P1 loop of dTASK6 was determined to play a role in proton sensing; however, full M1P1 chimeras were non-functional. Our own functional and potassium-selective chimeras now show that the differential pH sensitivity of TASK1 and TASK3 is due, in part, to the M1P1 loop. The presence of the TASK1 M1P1 loop (and hence a positively charged lysine at position 70) increases the pH sensitivity of TASK3 whereas the presence of the TASK3 M1P1 loop (and therefore introduction of a negatively charged

glutamate at position 70) decreases the pH sensitivity of the TASK1 channel.

TASK2 channels are highly sensitive to extracellular alkalinization (36), and an arginine at position 224 was recently reported to be the pH sensor of TASK2 channels (37). Mutation of charged residues within the M1P1 loop of TASK2 previously thought to form the pH sensor of these channels (8) leads to a shift of the pK_a by 0.6 pH units from a pK_a of 8 to ~7.4 (37). Niemeyer *et al.* (37) hypothesized that this anomalous shift may be due to structural changes or perhaps a partial collapse of the M1P1 loop. Our data, however, show similar shifts in pH sensitivity with M1P1 exchange between TASK1 and TASK3 channels, despite zinc sensitivity data demonstrating that there must be correct outer mouth structure in these chimeras. As such, our data suggest that the M1P1 loop of TASK channels has a more complex role to play in channel regulation than mere electrostatic effects at the outer mouth.

The only potassium channel family with a similarly long extracellular pre-pore loop as K2P channels is the ether-a-go-go (EAG) family. The best characterized member of this family is the human ether-a-go-go gene (HERG) potassium channel, which has a 42-amino acid pre-pore extracellular loop called the S5P linker. We and others have shown this linker forms an amphipathic α-helix that is critical for HERG channel regulation and likely to interact with the mouth of the pore, playing a central role in HERG rapid C-type-like inactivation (30, 38, 39). However, the positioning of this helical linker and the mechanism of this C-type-like inactivation are still unknown. K2P channels are also suggested to undergo C-type-like inactivation (40); indeed, it has been recently hypothesized that closure of both TASK2 and TASK1 channels upon extracellular pH changes is analogous to C-type-like inactivation (27, 37). Thus, in addition to influencing external regulation of these channels, the M1P1 loop may play a role in intrinsic K2P channel gating.

Acknowledgments—We thank Bill Wisden and Helen Meadows for the kind gifts of cDNA for TASK channels and Frank Döring for helpful discussion.

REFERENCES

1. Goldstein, S. A., Bockenhauer, D., O'Kelly, I., and Zilberberg, N. (2001) *Nat. Rev. Neurosci.* **2,** 175–184
2. O'Connell, A. D., Morton, M. J., and Hunter, M. (2002) *Biochim. Biophys. Acta* **1566,** 152–161
3. Lesage, F. (2003) *Neuropharmacology* **44,** 1–7
4. Kim, D. (2005) *Curr. Pharm. Des.* **11,** 2717–2736
5. Lotshaw, D. P. (2007) *Cell Biochem. Biophys.* **47,** 209–256
6. Lesage, F., Reyes, R., Fink, M., Duprat, F., Guillemare, E., and Lazdunski, M. (1996) *EMBO J.* **15,** 6400–6407
7. Morton, M. J., O'Connell, A. D., Sivaprasadarao, A., and Hunter, M. (2003) *Pflugers Arch. Eur. J. Physiol.* **445,** 577–583
8. Morton, M. J., Abohamed, A., Sivaprasadarao, A., and Hunter, M. (2005) *Proc. Natl. Acad. Sci. U. S. A.* **102,** 16102–16106
9. Döring, F., Scholz, H., Kühnlein, R. P., Karschin, A., and Wischmeyer, E. (2006) *Eur. J. Neurosci.* **24,** 2264–2274
10. Goldstein, S. A. N., Bayliss, D. A., Kim, D., Lesage, F., Plant, L. D., and Rajan, S. (2005) *Pharmacol. Rev.* **57,** 527–540
11. Alexander, S. P., Mathie, A., and Peters, J. A. (2008) *Br. J. Pharmacol.* **153,** Suppl. 2, S1–S209
12. Duprat, F., Lauritzen, I., Patel, A., and Honore, E. (2007) *Trends Neurosci.* **30,** 573–580
13. Mathie, A. (2007) *J. Physiol.* **578,** 377–385
14. Millar, J. A., Barratt, L., Southan, A. P., Page, K. M., Fyffe, R. E., Robertson, B., and Mathie, A. (2000) *Proc. Natl. Acad. Sci. U. S. A.* **97,** 3614–3618
15. Talley, E. M., Lei, Q., Sirois, J. E., and Bayliss, D. A. (2000) *Neuron* **25,** 399–410
16. Lauritzen, I., Zanzouri, M., Honore, E., Duprat, F., Ehrengruber, M. U., Lazdunski, M., and Patel, A. J. (2003) *J. Biol. Chem.* **278,** 32068–32076
17. Mathie, A., Clarke, C. E., Ranatunga, K. M., and Veale, E. L. (2003) *Cerebellum* **2,** 11–25
18. Kang, D., Han, J., Talley, E. M., Bayliss, D. A., and Kim, D. (2004) *J. Physiol.* **554,** 64–77
19. Aller, M. I., Veale, E. L., Linden, A. M., Sandu, C., Schwaninger, M., Evans, L. J., Korpi, E. R., Mathie, A., Wisden, W., and Brickley, S. G. (2005) *J. Neurosci.* **25,** 11455–11467
20. Brickley, S. G., Aller, M. I., Sandu, C., Veale, E. L., Alder, F. G., Sambi, H., Mathie, A., and Wisden, W. (2007) *J. Neurosci.* **27,** 9329–9340
21. Rajan, S., Wischmeyer, E., Xin Liu, G., Preisig-Müller, R., Daut, J., Karschin, A., and Derst, C. (2000) *J. Biol. Chem.* **275,** 16650–16657
22. Kim, Y., Bang, H., and Kim, D. (2000) *J. Biol. Chem.* **275,** 9340–9347
23. Lopes, C. M., Zilberberg, N., and Goldstein, S. A. (2001) *J. Biol. Chem.* **276,** 24449–24452
24. Clarke, C. E., Veale, E. L., Green, P. J., Meadows, H. J., and Mathie, A. (2004) *J. Physiol.* **560,** 51–62
25. Czirjak, G., and Enyedi, P. (2003) *Mol. Pharmacol.* **63,** 646–652
26. Musset, B., Meuth, S. G., Liu, G. X., Derst, C., Wegner, S., Pape, H. C., Budde, T., Preisig-Muller, R., and Daut, J. (2006) *J. Physiol.* **572,** 639–657
27. Yuill, K. H., Stansfeld, P. J., Ashmole, I., Sutcliffe, M. J., and Stanfield, P. R. (2007) *Pflugers Arch. Eur. J. Physiol.* **455,** 333–348
28. Careaga, C. L., and Falke, J. J. (1992) *Biophys. J.* **62,** 209–216
29. Laine, M., Lin, M. C., Bannister, J. P., Silverman, W. R., Mock, A. F., Roux, B., and Papazian, D. M. (2003) *Neuron* **39,** 467–481
30. Clarke, C. E., Hill, A. P., Zhao, J., Kondo, M., Subbiah, R. N., Campbell, T. J., and Vandenberg, J. I. (2006) *J. Physiol.* **573,** 291–304
31. Lopes, C. M., Gallagher, P. G., Buck, M. E., Butler, M. H., and Goldstein, S. A. (2000) *J. Biol. Chem.* **275,** 16969–16978
32. Mathie, A., Sutton, G. L., Clarke, C. E., and Veale, E. L. (2006) *Pharmacol. Ther.* **111,** 567–583
33. Krezel, A., Lesniak, W., Jezowska-Bojczuk, M., Mlynarz, P., Brasun, J., Kozlowski, H., and Bal, W. (2001) *J. Inorg. Biochem.* **84,** 77–88
34. Sobolevsky, A. I., Yelshansky, M. V., and Wollmuth, L. P. (2004) *Neuron* **41,** 367–378
35. Yuill, K., Ashmole, I., and Stanfield, P. R. (2004) *Pflugers Arch. Eur. J. Physiol.* **448,** 63–69
36. Reyes, R., Duprat, F., Lesage, F., Fink, M., Salinas, M., Farman, N., and Lazdunski, M. (1998) *J. Biol. Chem.* **273,** 30863–30869
37. Niemeyer, M. I., Gonzalez-Nio, F. D., Zuniga, L., Gonzalez, W., Cid, L. P., and Sepulveda, F. V. (2007) *Proc. Natl. Acad. Sci. U. S. A.* **104,** 666–671
38. Liu, J., Zhang, M., Jiang, M., and Tseng, G. N. (2002) *J. Gen. Physiol.* **120,** 723–737
39. Torres, A. M., Bansal, P. S., Sunde, M., Clarke, C. E., Bursill, J. A., Smith, D. J., Bauskin, A., Breit, S. N., Campbell, T. J., Alewood, P. F., Kuchel, P. W., and Vandenberg, J. I. (2003) *J. Biol. Chem.* **278,** 42136–42148
40. Zilberberg, N., Ilan, N., and Goldstein, S. A. N. (2001) *Neuron* **32,** 635–648